

This discussion paper is/has been under review for the journal Geoscientific Model Development (GMD). Please refer to the corresponding final paper in GMD if available.

Implementation of a soil albedo scheme in the CABLEv1.4b land surface model and evaluation against MODIS estimates over Australia

J. Kala¹, J. P. Evans¹, A. J. Pitman¹, C. B. Schaaf², M. Decker¹, C. Carouge¹, D. Mocko³, and Q. Sun²

¹Australian Research Council Centre of Excellence for Climate Systems Science and Climate Change Research Centre, University of New South Wales, Sydney, NSW, 2052, Australia

³SAIC at NASA Goddard Space Flight Centre, NASA, Greenbelt, MD, USA

²Department of Earth and the Environment, Boston University, Boston, Massachusetts, USA

Received: 23 January 2014 – Accepted: 5 March 2014 – Published: 13 March 2014

Correspondence to: J. Kala (j.kala@unsw.edu.au, jatin.kala.jk@gmail.com)

Published by Copernicus Publications on behalf of the European Geosciences Union.

1671

Abstract

Land surface albedo, the fraction of incoming solar radiation reflected by the land surface, is a key component of the earth system. This study evaluates snow-free surface albedo simulations by the Community Atmosphere Biosphere Land Exchange (CABLEv1.4b) model with the Moderate Resolution Imaging Spectroradiometer (MODIS) albedo. We compare results from two offline simulations over the Australian continent, one with prescribed background snow-free and vegetation-free soil albedo derived from MODIS (the control), and the other with a simple parameterisation based on soil moisture and colour. The control simulation shows that CABLE simulates albedo over Australia reasonably well, with differences with MODIS within an acceptable range. Inclusion of the parameterisation for soil albedo however introduced large errors for the near infra red albedo, especially for desert regions of central Australia. These large errors were not fully explained by errors in soil moisture or parameter uncertainties, but are similar to errors in albedo in other land surface models which use the same soil albedo scheme. Although this new parameterisation has introduced larger errors as compared to prescribing soil albedo, dynamic soil moisture-albedo feedbacks are now enabled in CABLE. Future directions for albedo parameterisations development in CABLE are discussed.

1 Introduction

The albedo of the land surface is the ratio of upwelling to downwelling shortwave radiation and determines the fraction of incoming solar radiation reflected back to the atmosphere. It is one of the key drivers of the earth's climate as it determines, in part, the amount of energy available to drive processes in the atmosphere and the land surface (e.g., Dickinson, 1983). Hence, the incorrect prescription or parameterisation of surface albedo can result in large model biases. Therefore, the correct representation

1672

of albedo in land surface models (LSMs), whether prescribed or parameterised, is of critical importance to the surface energy and hydrological cycle.

The overall albedo of the land is a function of the vegetation, soil, and snow albedos. The main factor which determines which of these three albedos has the strongest influence on the overall surface albedo is the fractional area covered by each of vegetation, soil and snow. These are commonly parameterised as a function of leaf area index (LAI), the total one-sided surface area of leaf per ground surface area (Bonan, 2008). When LAI is high, most of the incoming solar energy is reflected, scattered, and/or absorbed by the vegetation canopy and only a small proportion of radiation reaches the ground and the overall albedo is primarily that of the vegetation canopy. When LAI is small, the converse is true and the overall albedo is primarily that of the soil or snow.

Vegetation albedo is a function of the radiative properties of the canopy, i.e., the leaf transmittance and reflectance, as well its physical properties, namely, the leaf angle or orientation, canopy clumping and structure. Leaf transmittance and reflective properties determine how much radiation penetrates through the canopy and are usually prescribed in LSMs for each plant functional type (PFT) in the visible (VIS, 0.4–0.7 μm) and near infra-red (NIR, 0.7–4.0 μm) bands. This distinction is important since green canopies absorb most of the solar radiation in the VIS waveband for photosynthesis, but reflect and transmit most of the radiation in the NIR waveband (Bonan, 2008). Leaf structural and physical properties can also influence within-canopy shadowing, which allows higher exposure of the underlying soil and/or snow cover, especially in low density forests (Davidson and Wang, 2004). Leaf orientation influences albedo since the maximum incident solar radiation on a leaf occurs when the beam is perpendicular to the surface (Bonan, 2008).

Soil albedo is a function of soil colour, determined partly by its organic composition, and more importantly, soil moisture, with saturated soils generally having lower albedo than dry soils (Idso et al., 1975). This is especially important in transitional climatic regions, where significant soil moisture variability drives strong land–atmosphere coupling (e.g., Koster et al., 2004). Although the dependence of soil albedo on soil moisture

1673

has been well established from field experiments (e.g., Idso et al., 1975), several LSMs do not include this feedback and recent studies have shown that it plays an important role in seasonal droughts in the central US (Zaitchik et al., 2012). Recent studies over eastern Australia have shown that the use of time-varying MODIS albedo as opposed to monthly mean climatologies from AVHRR in a regional climate model improved mean air temperature simulations, and to a lesser extent, precipitation (Meng et al., 2013). This was particularly evident in arid regions, where the overall albedo is predominantly influenced by soil rather than vegetation.

Vegetation and soil albedo are also influenced by the solar zenith angle, especially in desert regions (Wang et al., 2005). This only applies under clear-sky conditions (i.e., direct beam radiation) when there is little or no scattering of the incoming shortwave radiation. In the morning just after sunrise and late afternoon before sunset, albedo is generally higher, as compared to mid-day when the sun is directly overhead. The inclusion of soil and vegetation albedo dependence on solar zenith angle during clear-sky conditions has improved albedo simulations in some LSMs (Liang et al., 2005).

With recent developments in satellite remote sensing, several surface albedo products are now available at a high spatial and temporal resolution and spanning several years. This has allowed for the careful evaluation of albedo in various LSMs (e.g., Wei et al., 2001; Oleson et al., 2003; Zhou et al., 2003; Wang et al., 2004); the development of vegetation and soil albedo parameterisations (e.g., Liang et al., 2005; Yang et al., 2008); as well as the mapping of land surface parameters such as the spatial and temporal distribution of PFTs, LAI and soil color, for use in LSMs (Lawrence and Chase, 2007). Clearly, the use of satellite remote sensing can be very useful in both the evaluation and development of LSMs.

This paper focusses on the Community Atmosphere Biosphere Land Exchange (CABLE) model (Wang et al., 2011), an LSM designed to simulate fluxes of heat, moisture, and carbon at the land surface. While several studies have used CABLE (e.g., Cruz et al., 2010; Zhang et al., 2011; Pitman et al., 2011; Wang et al., 2012; Exbrayat et al., 2012), no studies have explicitly examined simulations of surface albedo. The aim of

1674

in Fig. 9 showing a monthly times series of observed and simulated net radiation, sensible heat and latent heat flux at the Howard-Springs (HS) and Tumberumba (TB) sites (Fig. 2b). Only the CNTL experiment is plotted as both simulations had very similar fluxes, as they are not located in regions where the differences between the CNTL and PSALB experiments were large. The RMSEs and biases for both simulations at both sites is summarised in Table 4, which shows only small differences between the two simulations. However, it is still useful to examine the performance of the model. CABLE systematically underestimates net radiation at the HS site, but performs remarkably well at the TB site. This may not be un-expected as the TB site experiences a temperate climate, with a clear seasonal cycle in the observed net radiation, whereas the HS site is close to the tropics and does not have such a clear seasonal signal. This systematic under prediction of net radiation could not be directly explained by the errors in albedo (Fig. 4).

4 Discussion

The CABLE land surface model prescribes background soil albedo and hence does not allow for soil moisture-albedo feedbacks, which the literature suggests can be important. To address this issue, we implemented a simple soil albedo scheme, based on soil moisture and colour, which has been commonly used in other LSMs. Two simulations were conducted, one with prescribed soil albedo derived from MODIS, the control (CNTL) experiment, and another with parameterised soil albedo (PSALB). The CNTL simulation showed relatively small errors in albedo when compared to MODIS whereas the PSALB experiment showed much larger errors especially in the VIS albedo. The differences were up to -0.25 and mainly in central Australia. The better performance of the CNTL as compared to PSALB is not surprising as the CNTL experiment uses a background soil albedo which is itself derived from earlier versions of MODIS albedo (Houldcroft et al., 2009). The large errors in the NIR albedo in the desert regions of Australia has been found elsewhere. Wang et al. (2004) compared albedo simulations

1683

globally from the CLM2 LSM against MODIS and also found similar large errors in the NIR albedo in central Australia (see Fig. 5c in Wang et al., 2004). Numerous other studies have also found that the largest errors in NIR albedo from LSMs tend to be in desert and arid regions such as the Sahara (Wei et al., 2001; Oleson et al., 2003; Zhou et al., 2003; Wang et al., 2004). The much larger errors for the NIR as compared to the VIS albedo as found in this study has also been reported by Wang et al. (2004). This is due to the fact that NIR albedos over snow-free surfaces are larger in magnitude than the VIS albedo, and hence, likely to show larger error.

Given the large errors in albedo between MODIS and LSMs, Lawrence and Chase (2007) developed MODIS-consistent land-surface parameters, including the mapping of PFTs, LAI, and soil color for use within the CLM3 LSM. They clearly demonstrated that the use of the modified parameter maps improved surface albedo simulations when compared against MODIS albedo, which in some instances, resulted in improved simulations of precipitation and near-surface temperature. However the process of generating new soil colour maps involved the fitting of VIS and NIR albedos for each grid cell to reproduce values from MODIS, and then using the model soil moisture to re-compute corresponding soil colours. Hence, although a similar method could be applied using CABLE, this would lead to model-specific parameter mapping of a physical soil property for which there is no logical reason why it (soil colour) should be different across models. In the longer term, such an approach could lead to unnecessary complexity. Comparing the performance of models that have calibrated soil color adds a degree of unnecessary complexity that can be avoided by using observed soil color. The use of more accurate PFT maps however is more straight-forward, and examination of the MODIS MOD12C1 PFT yearly classification showed that the area of barren land in central Australia from 2001 to present is generally larger as compared to what is used for the simulations as shown in Fig. 2a. However, running CABLE with MOD12C1 yearly varying PFT maps (not shown) did not result in marked changes in albedo simulations as compared to MODIS.

1684

The errors in albedo in central Australia are also likely due to inherent limitations of the parameterisation in Eq. (2), which was originally developed for the BATS LSM (Dickinson et al., 1993), adopted in CLM, and now in CABLE. Equation (2) is based on an absolute soil moisture value and this presents issues with regards to the universal application of the scheme irrespective of LSM, as the latter vary considerably in their treatment of soil moisture (Koster et al., 2009), as well as the processes which influence soil moisture (Koster and Milly, 1997). Specifically, the volumetric soil moisture simulated between LSMs is not transferable, rather it is a model-specific state that reflects the integration of many processes. These can be substantially avoided if future parameterisation are developed using soil wetness. This is a dimensionless index defined between extremes such as zero soil water, wilting point, field capacity, and saturation level, rather than soil moisture expressed as a volume of water. This issue is well known in the LSM community and was discussed in detail by Dirmeyer (2011). Another limitation is the 8 generic soil colour classes used, as well as the assumption that the ratio of the NIR to VIS albedo is exactly a factor of 2. However, Wang et al. (2005) have shown that this ratio from MODIS data over the arid part of central Australia is 2.69.

The cause of the large differences between LSM simulated and observed albedo in arid regions is the well established dependence of soil albedo on solar zenith angle (Wang et al., 2005; Yang et al., 2008), and the lack of explicit physical representation of this relationship in many LSMs. Wang et al. (2005) devised a semi-empirical scheme to relate bare soil albedo at a single site in the Sahel to solar zenith angle, and show improvements in albedo and surface flux simulations when applied to the NOAH land surface model. However, their simulations were at the site-scale, and over a very short time-frame (less than 2 months) and may not be easily applicable to regional or global simulations over longer time-frames. Liang et al. (2005) however, developed a so called "dynamic-statistical" parameterisation of snow-free albedo using MODIS albedo and soil moisture from a land data assimilation system over north America. Whilst the dynamical part of the model represents physical dependencies on solar zenith angle and

1685

surface soil moisture etc., the statistical model provides parameter estimates specific to geographic location. This scheme has been shown to significantly improve albedo simulations in CLM over North America. A similar method could be adopted in CABLE in the future given we have identified this as a significant limitation of the model.

5 Conclusions

Surface albedo is a key element of the surface energy balance as it determines the amount of solar energy absorbed at the surface and re-distributed into sensible and latent heat, which in turn drive the surface energy and water cycles. In this study, we investigated how well CABLEv1.4b simulates albedo compared with MODIS estimates. We also tested a new simple parameterisation for the soil albedo, which is otherwise prescribed and held constant in time. This is an important step for the model as it enables the feedback between albedo and soil moisture to be represented. Our results show that CABLEv1.4b simulates overall albedo reasonably well when the soil albedo is prescribed as would be expected. The new parameterisation for soil albedo based on soil colour and soil moisture introduces large errors in the NIR albedo, especially in desert regions. These errors cannot be completely attributed to errors in soil moisture, or parameter uncertainties, but likely due to a lack of physical representation of zenith angle dependence of desert albedo. Hence, future development in CABLE albedo parameterisation should focus on incorporating this dependence and the work of Liang et al. (2005) provides a starting point in this direction. We also note that soil albedo parameterisations that use volumetric soil moisture, while entirely legitimate for the LSM they are designed for, are not easily transferable between LSMs. We recommend that future developments of soil albedo are based on the soil wetness, a quantity that is more transferable between models.

1686

- Idso, S. B., Jackson, R. D., Reginato, R. J., Kimball, B. A., and Nakayama, F. S.: The dependence of bare soil albedo on soil water content, *J. Appl. Meteorol.*, 14, 109–113, 1975. 1673, 1674
- Jones, D., Wang, W., and Fawcett, R.: High-quality spatial climate data-sets for Australia, *Aust. Meteorol. Mag.*, 58, 233–248, 2009. 1678
- 5 Kala, J., Decker, M., Exbrayat, J.-F., Pitman, A. J., Carouge, C., Evans, J. P., Abramowitz, G., and Mocko, D.: Influence of leaf area index prescriptions on simulations of heat, moisture, and carbon fluxes, *J. Hydrometeorol.*, 15, 489–503, doi:10.1175/JHM-D-13-063.1, 2013. 1675
- 10 Keeling, C. D., Piper, S. C., Bacastow, R. B., Wahlen, M., Whorf, T. P., Heimann, M., and Meijer, H. A.: Atmospheric CO₂ and ¹³CO₂ exchange with the terrestrial biosphere and oceans from 1978 to 2000: observations and carbon cycle implications, in: *A History of Atmospheric CO₂ and its effects on Plants, Animals, and Ecosystems*, edited by: Ehleringer, J. R., Cerling, T. E., and Dearing, M. D., Springer Verlag, New York, 83–113, 2005. 1678
- 15 Koster, R. D. and Milly, P. C. D.: The interplay between transpiration and runoff formulations in land surface schemes used with atmospheric models, *J. Climate*, 10, 1578–1591, 1997. 1685
- Koster, R. D., Guo, Z., Dirmeyer, P. A., Bonan, G., Chan, E., Cox, P., Davies, H., Gordon, C. T., Kanae, S., Kowalczyk, E., Lawrence, D., Liu, P., Lu, C.-H., Malyshev, S., McAvaney, B., Mitchell, K., Mocko, D., Oki, T., Oleson, K. W., Pitman, A., Sud, Y. C., Taylor, C. M.,
- 20 Versegny, D., Vasic, R., Xue, Y., and Yamada, T.: Regions of strong coupling between soil moisture and precipitation, *Science*, 305, 1138–1140, 2004. 1673
- Koster, R. D., Guo, Z., Yang, R., Dirmeyer, P. A., Mitchell, K., and Puma, M. J.: On the nature of soil moisture in land surface models, *J. Climate*, 22, 4322–4335, 2009. 1685
- Kowalczyk, E. A., Wang, Y. P., Law, R. M., Davies, H. L., McGregor, J. L., and Abramowitz, G.:
- 25 The CSIRO Atmosphere Biosphere Land Exchange model for use in climate models and as an offline model, Commonwealth Scientific and Industrial Research Organisation Marine and Atmospheric Research Paper 013, November 2006, available online: www.cmar.csiro.au/e-print/open/kowalczyka_2006a.pdf (last access: 10 November 2011), 37 pp., 2006. 1675
- 30 Kumar, S., Peters-Lidard, C., Tian, Y., Houser, P., Geiger, J., Olden, S., Lighty, L., Eastman, J., Doty, B., Dirmeyer, P., Adams, J., Mitchell, K., Wood, E., and Sheffield, J.: Land information system: an interoperable framework for high resolution land surface modeling, *Environ. Modell. Softw.*, 21, 1402–1415, 2006. 1677

1691

- Kumar, S. V., Peters-Lidard, C. D., Eastman, J. L., and Tao, W.-K.: An integrated high-resolution hydrometeorological modeling testbed using LIS and WRF, *Environ. Modell. Softw.*, 23, 169–181, 2008. 1677
- Lawrence, P. J. and Chase, T. N.: Representing a new MODIS consistent land surface
- 5 in the Community Land Model (CLM 3.0), *J. Geophys. Res.-Biogeo.*, 112, G01023, doi:10.1029/2006JG000168, 2007. 1674, 1684
- Liang, X.-Z., Xu, M., Gao, W., Kunkel, K., Slusser, J., Dai, Y., Min, Q., Houser, P. R., Rodell, M., Schaaf, C. B., and Gao, F.: Development of land surface albedo parameterization based on
- 10 Moderate Resolution Imaging Spectroradiometer (MODIS) data, *J. Geophys. Res.-Atmos.*, 110, D11107, doi:10.1029/2004JD005579, 2005. 1674, 1685, 1686
- Liu, Y. Y., van Dijk, A. I. J. M., de Jeu, R. A. M., and Holmes, T. R. H.: An analysis of spatiotemporal variations of soil and vegetation moisture from a 29-year satellite-derived data set over mainland Australia, *Water Resour. Res.*, 45, W07405, doi:10.1029/2008WR007187, 2009. 1680
- 15 Lucht, W., Schaaf, C., and Strahler, A.: An algorithm for the retrieval of albedo from space using semi-empirical BRDF models, *IEEE T. Geosci. Remote*, 38, 977–998, 2000. 1679
- Mao, J., Phipps, S. J., Pitman, A. J., Wang, Y. P., Abramowitz, G., and Pak, B.: The CSIRO Mk3L climate system model v1.0 coupled to the CABLE land surface scheme v1.4b: evaluation of the control climatology, *Geosci. Model Dev.*, 4, 1115–1131, doi:10.5194/gmd-4-1115-2011, 2011. 1675
- 20 Meng, X., Evans, J., and McCabe, M.: The influence of inter-annually varying albedo on regional climate and drought, *Clim. Dynam.*, 42, 787–803, doi:10.1007/s00382-013-1790-0, 2013. 1674
- Oleson, K. W., Bonan, G. B., Schaaf, C., Gao, F., Jin, Y., and Strahler, A.: Assessment of global climate model land surface albedo using MODIS data, *Geophys. Res. Lett.*, 30, 1443, doi:10.1029/2002GL0167498, 2003. 1674, 1679, 1684
- 25 Pitman, A. J., Avila, F. B., Abramowitz, G., Wang, Y. P., Phipps, S. J., and de Noblet-Ducoudré, N.: Importance of background climate in determining impact of land-cover change on regional climate, *Nature Climate Change*, 9, 472–475, 2011. 1674, 1679
- 30 Raupach, M. R.: Simplified expressions for vegetation roughness length and zero-plane displacement as functions of canopy height and area index, *Bound.-Lay. Meteorol.*, 71, 211–216, 1994. 1675

1692

- Rienecker, M. M., Suarez, M. J., Gelaro, R., Todling, R., Bacmeister, J., Liu, E., Bosilovich, M. G., Schubert, S. D., Takacs, L., Kim, G.-K., Bloom, S., Chen, J., Collins, D., Conaty, A., da Silva, A., Gu, W., Joiner, J., Koster, R. D., Lucchesi, R., Molod, A., Owens, T., Pawson, S., Pegion, P., Redder, C. R., Reichle, R., Robertson, F. R., Ruddick, A. G., Sienkiewicz, M., and Woollen, J.: MERRA: NASA's Modern-Era Retrospective Analysis for Research and Applications, *J. Climate*, 24, 3624–3648, 2011. 1678
- Schaaf, C. B., Gao, F., Strahler, A. H., Lucht, W., Li, X., Tsang, T., Strugnell, N. C., Zhang, X., Jin, Y., Muller, J.-P., Lewis, P., Barnsley, M., Hobson, P., Disney, M., Roberts, G., Dunderdale, M., Doll, C., d'Entremont, R. P., Hu, B., Liang, S., Privette, J. L., and Roy, D.: First operational BRDF, albedo nadir reflectance products from MODIS, *Remote Sens. Environ.*, 83, 135–148, 2002. 1679
- Spitters, C.: Separating the diffuse and direct component of global radiation and its implications for modeling canopy photosynthesis Part II. Calculation of canopy photosynthesis, *Agr. Forest Meteorol.*, 38, 231–242, 1986. 1676
- Tsvetsinskaya, E. A., Schaaf, C. B., Gao, F., Strahler, A. H., Dickinson, R. E., Zeng, X., and Lucht, W.: Relating MODIS-derived surface albedo to soils and rock types over Northern Africa and the Arabian peninsula, *Geophys. Res. Lett.*, 29, D20106, doi:10.1029/2005JD006772, 2002. 1677
- Vamborg, F. S. E., Brovkin, V., and Claussen, M.: The effect of a dynamic background albedo scheme on Sahel/Sahara precipitation during the mid-Holocene, *Clim. Past*, 7, 117–131, doi:10.5194/cp-7-117-2011, 2011. 1677
- Wang, Y.-P. and Leuning, R.: A two-leaf model for canopy conductance, photosynthesis and partitioning of available energy I: Model description and comparison with a multi-layered model, *Agr. Forest Meteorol.*, 91, 89–111, 1998. 1675
- Wang, Y. P., Kowalczyk, E., Leuning, R., Abramowitz, G., Raupach, M. R., Pak, B., van Gorsel, E., and Luhar, A.: Diagnosing errors in a land surface model (CABLE) in the time and frequency domains, *J. Geophys. Res.*, 116, G01034, doi:10.1029/2010JG001385, 2011. 1674, 1675
- Wang, Y. P., Lu, X. J., Wright, I. J., Dai, Y. J., Rayner, P. J., and Reich, P. B.: Correlations among leaf traits provide a significant constraint on the estimate of global gross primary production, *Geophys. Res. Lett.*, 39, L19405, doi:10.1029/2012GL053461, 2012. 1674

1693

- Wang, Z., Zeng, X., Barlage, M., Dickinson, R. E., Gao, F., and Schaaf, C. B.: Using MODIS BRDF and albedo data to evaluate global model land surface albedo, *J. Hydrometeorol.*, 5, 3–14, 2004. 1674, 1677, 1679, 1683, 1684
- Wang, Z., Barlage, M., Zeng, X., Dickinson, R. E., and Schaaf, C. B.: The solar zenith angle dependence of desert albedo, *Geophys. Res. Lett.*, 32, L05403, doi:10.1029/2004GL021835, 2005. 1674, 1685
- Wang, Z., Schaaf, C. B., Strahler, A. H., Chopping, M. J., Roman, M. O., Shuai, Y., Woodcock, C. E., Hollinger, D. Y., and Fitzjarrald, D. R.: Evaluation of MODIS albedo product (MCD43A) over grassland, agriculture and forest surface types during dormant and snow-covered periods, *Remote Sens. Environ.*, 140, 60–77, 2014. 1679
- Wei, X., Hahmann, A. N., Dickinson, R. E., Yang, Z.-L., Zeng, X., Schaudt, K. J., Schaaf, C. B., and Strugnell, N.: Comparison of albedos computed by land surface models and evaluation against remotely sensed data, *J. Geophys. Res.-Atmos.*, 106, 20687–20702, 2001. 1674, 1684
- Yang, F., Mitchell, K., Hou, Y.-T., Dai, Y., Zeng, X., Wang, Z., and Liang, X.-Z.: Dependence of land surface albedo on solar zenith angle: observations and model parameterization, *J. Appl. Meteorol. Clim.*, 47, 2963–2982, 2008. 1674, 1685
- Yuan, H., Dai, Y., Xiao, Z., Ji, D., and Shangguan, W.: Reprocessing the MODIS Leaf Area Index products for land surface and climate modelling, *Remote Sens. Environ.*, 115, 1171–1187, 2011. 1678, 1701
- Zaitchik, B. F., Santanello, J. A., Kumar, S. V., and Peters-Lidard, C. D.: Representation of soil moisture feedbacks during drought in NASA Unified WRF (NU-WRF), *J. Hydrometeorol.*, 14, 360–367, doi:10.1175/JHM-D-12-069.1, 2012. 1674, 1677
- Zeng, X., Shaikh, M., Dai, Y., Dickinson, R. E., and Myneni, R.: Coupling of the Common Land Model to the NCAR Community Climate Model, *J. Climate*, 15, 1832–1854, 2002. 1677
- Zhang, Q., Wang, Y. P., Pitman, A. J., and Dai, Y. J.: Limitations of nitrogen and phosphorous on the terrestrial carbon uptake in the 20th century, *Geophys. Res. Lett.*, 38, L22701, doi:10.1029/2011GL049244, 2011. 1674
- Zhou, L., Dickinson, R. E., Tian, Y., Zeng, X., Dai, Y., Yang, Z.-L., Schaaf, C. B., Gao, F., Jin, Y., Strahler, A., Myneni, R. B., Yu, H., Wu, W., and Shaikh, M.: Comparison of seasonal and spatial variations of albedos from Moderate-Resolution Imaging Spectroradiometer (MODIS) and Common Land Model, *J. Geophys. Res.-Atmos.*, 108, 4488, doi:10.1029/2002JD003326, 2003. 1674, 1679, 1684

1694

Table 1. Names of plant functional types (PFTs) and soil types shown in Fig. 2a.

| PFT number | PFT |
|------------|----------------------|
| 1 | Evergreen Needleleaf |
| 2 | Evergreen Broadleaf |
| 3 | Deciduous Needleleaf |
| 4 | Deciduous Broadleaf |
| 5 | Mixed Forest |
| 6 | Closed Shrublands |
| 7 | Open Shrublands |
| 8 | Woody Savannas |
| 9 | Savannas |
| 10 | Grasslands |
| 11 | Permanent Wetlands |
| 12 | Croplands |
| 13 | Urban and Built-up |
| 14 | Cropland Mosaics |
| 15 | Snow and Ice |
| 16 | Barren |

1695

Table 2. Saturated and dry soil albedos for different soil colours (Fig. 2c) in the VIS and NIR wavebands.

| Soil Color | α_{sat} | | α_{dry} | |
|------------|-----------------------|------|-----------------------|------|
| | NIR | VIS | NIR | VIS |
| 1 | 0.12 | 0.24 | 0.24 | 0.48 |
| 2 | 0.11 | 0.22 | 0.22 | 0.44 |
| 3 | 0.10 | 0.20 | 0.20 | 0.40 |
| 4 | 0.09 | 0.18 | 0.18 | 0.36 |
| 5 | 0.08 | 0.16 | 0.16 | 0.32 |
| 6 | 0.07 | 0.14 | 0.14 | 0.28 |
| 7 | 0.06 | 0.12 | 0.12 | 0.24 |
| 8 | 0.05 | 0.10 | 0.10 | 0.20 |

1696

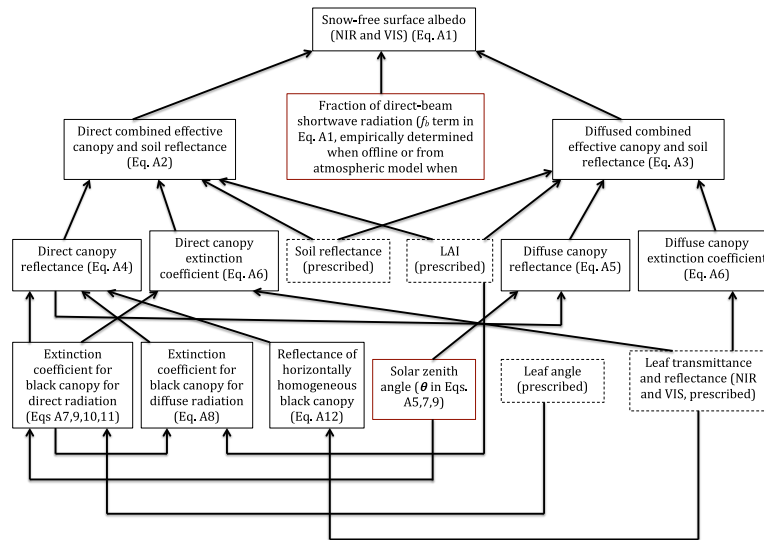


Fig. 1. Schematic illustration of snow-free surface albedo parameterisation in CABLE. Boxes with dashed lines represent user-defined input parameters to the model. The boxes with solid black lines represent the equations described in Appendix A and the boxes in solid red lines represent terms used in the equations.

1699

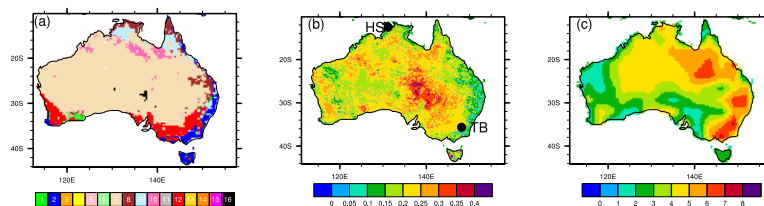


Fig. 2. (a) Distribution of PFTs in the domain, (b) prescribed background snow-free soil albedo from Houldcroft et al. (2009) used in the CNTL experiment, and (c) soil colours used in the PSALB experiment. The black dots in panel (b) represent the station location of the Howard-Springs (HS) and Tumberumba (TB) FLUXNET sites described in Sect. 2.4. The PFTs in panel (a) are shown in Table 1.

1700

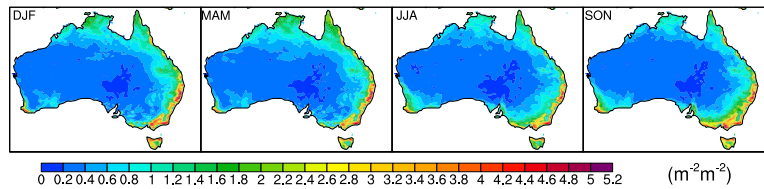


Fig. 3. Seasonal mean LAI from Yuan et al. (2011) (monthly means are used in the simulations).

1701

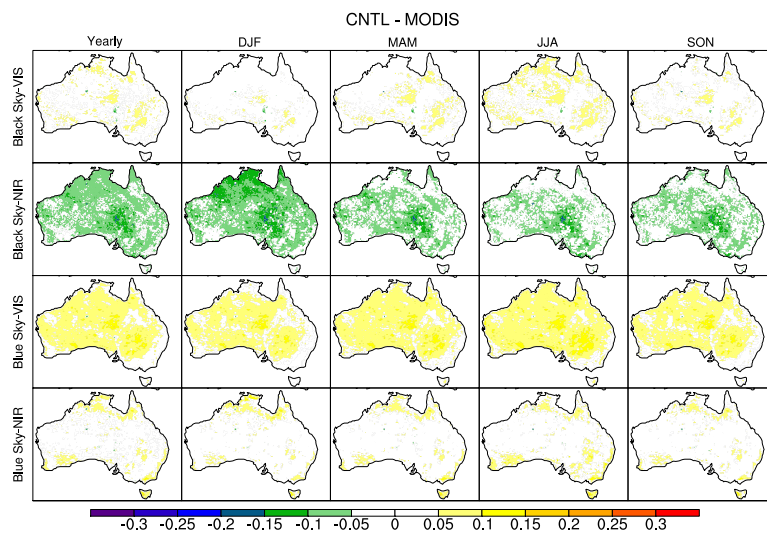


Fig. 4. Mean yearly and seasonal differences between CNTL and MODIS albedo (CNTL-MODIS) over the period 2001–2008. December-January-February (DJF) is summer, March-April-May (MAM) is autumn, June-July-August (JJA) is winter, September-October-November (SON) is spring.

1702

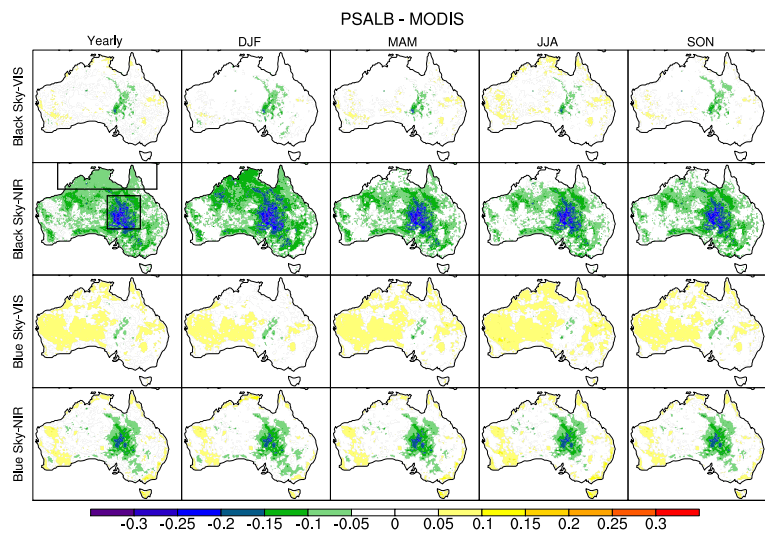


Fig. 5. Same as in Fig. 4, except for the PSALB experiment (PSALB-MODIS). The northern and central boxes in the Black Sky-NIR yearly panel show the regions from which a time-series is plotted in Fig. 6.

1703

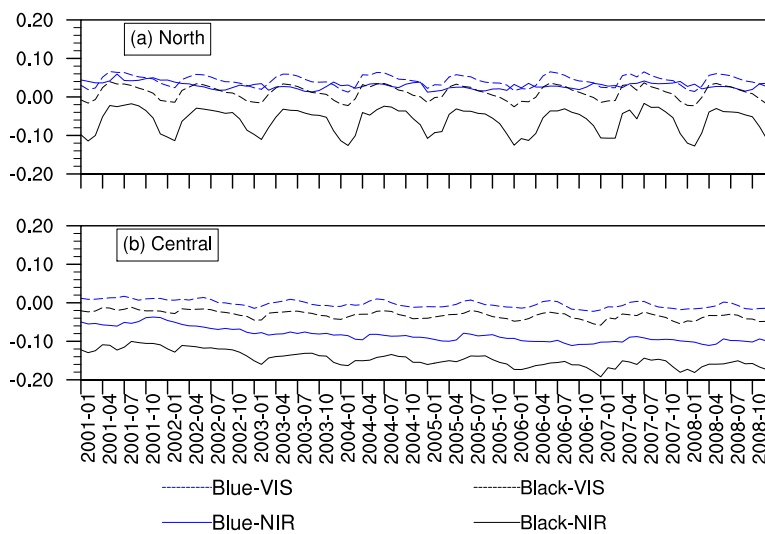


Fig. 6. Monthly time series of difference between PSALB and MODIS (PSALB-MODIS) spatially averaged over the northern and central boxes shown in the Black Sky-NIR yearly panel in Fig. 5.

1704

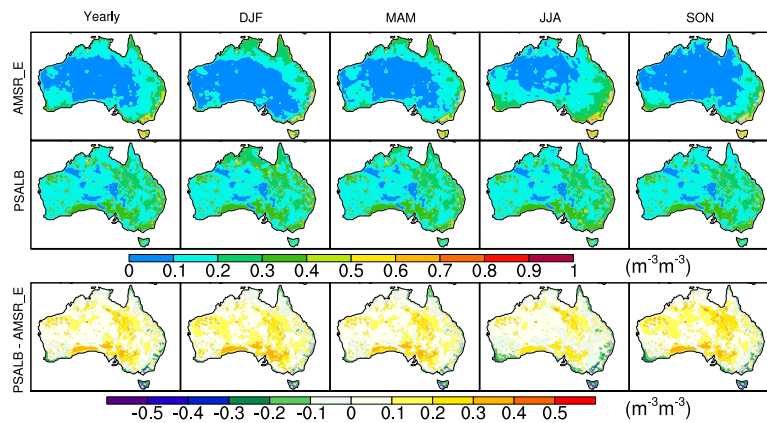


Fig. 7. Yearly and seasonal soil moisture from AMSR-E, the PSALB experiment, and difference between PSALB and AMSR-E (PSALB-AMSR_E).

1705

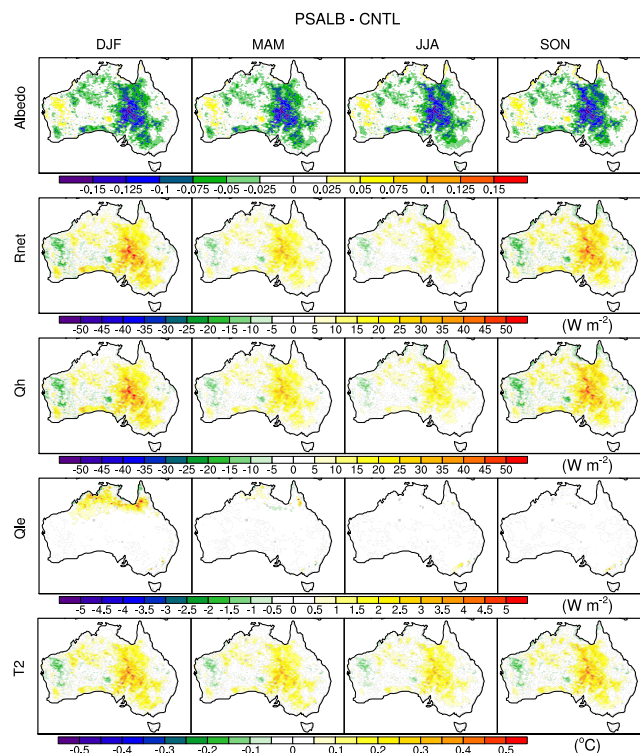


Fig. 8. Seasonal differences in albedo, net radiation (Rnet), sensible heat (Qh), latent heat (Qle) flux and screen level derived temperature (T2) between the PSALB and CNTL experiments (PSALB-CNTL).

1706

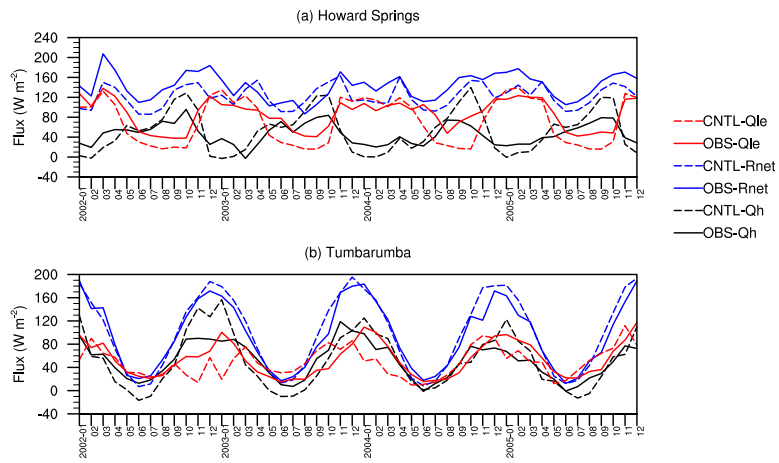


Fig. 9. Time series of mean monthly observed (solid lines) and CNTL (dotted lines) net radiation (blue), sensible heat flux (black), and latent heat flux (red) at **(a)** the Howard Springs, and **(b)** Tumarumba sites (Fig. 2b).